Publ. Astron. Soc. Japan (2014) 00(0), 1–9
doi: 10.1093/pasj/xxx000

arXiv:1511.09424v2 [astro-ph.HE] 8 Dec 2015

Iron Fluorescent Line Emission from the mCvs and Hard X-ray Emitting Symbiotic Stars as a Source of the Iron Fluorescent Line Emission from the Galactic Ridge

Romanus EZE,[1,2] **Kei SAITOU,**[1,3] **and Ken EBISAWA**[1,3]

[1]Japan Aerospace Exploration Agency, Institute of Space and Astronautical Science, 3-1-1 Yoshinodai, Chuo-ku, Sagamihara, Kanagawa 252-5210
[2]Department of Physics and Astronomy, University of Nigeria, Nsukka, Nigeria
[3]Department of Astronomy, Graduate School of Science, The University of Tokyo, 7-3-1 Hongo, Bunkyo-ku, Tokyo 113-0033

*E-mail: eze@ac.jaxa.jp or romanus.eze@unn.edu.ng

Received ⟨February 9, 2012⟩; Accepted ⟨acception date⟩

Abstract

The Galactic Ridge X-ray Emission (GRXE) spectrum has strong iron emission lines at 6.4, 6.7, and 7.0 keV, each corresponding to the neutral (or low-ionized), He-like, and H-like iron ions. The 6.4 keV fluorescence line is due to irradiation of neutral (or low ionized) material (iron) by hard X-ray sources, indicating uniform presence of the cold matter in the Galactic plane. In order to resolve origin of the cold fluorescent matter, we examined the contribution of the 6.4 keV line emission from white dwarf surfaces in the hard X-ray emitting symbiotic stars (hSSs) and magnetic cataclysmic variables (mCVs) to the GRXE. In our spectral analysis of 4 hSSs and 19 mCVs observed with Suzaku, we were able to resolve the three iron emission lines. We found that the equivalent-widths (EWs) of the 6.4 keV lines of hSSs are systematically higher than those of mCVs, such that the average EWs of hSSs and mCVs are 179^{+46}_{-11} eV and 93^{+20}_{-3} eV, respectively. The EW of hSSs compares favorably with the typical EWs of the 6.4 keV line in the GRXE of 90–300 eV depending on Galactic positions. Average 6.4 keV line luminosities of the hSSs and mCVs are 9.2×10^{39} and 1.6×10^{39} photons s^{-1}, respectively, indicating that hSSs are intrinsically more efficient 6.4 keV line emitters than mCVs. We compare expected contribution of the 6.4 keV lines from mCVs with the observed GRXE 6.4 keV line flux in the direction of $(l,b) \approx (28.5^\circ, 0^\circ)$. We conclude that almost all the 6.4 keV line flux in GRXE may be explained by mCVs within current undertainties of the stellar number densities, while contribution from hSSs may not be negligible.

Key words: Galaxy: disk — stars: binaries: symbiotic — stars: novae, cataclysmic variables — X-rays: stars

1 Introduction

Presence of the seemingly extended hard X-ray emission from the Galactic Ridge has been known since early 1980's (Galactic Ridge X-ray Emission; GRXE: Worrall et al. 1982; Warwick et al. 1985; Koyama et al. 1986). Strong iron K-line emission at ∼6.7 keV in the GRXE indicates its thermal plasma origin (e.g., Koyama et al. 1986; Yamauchi & Koyama 1993). More precise iron line diagnostics of the GRXE has been made possible

© 2014. Astronomical Society of Japan.

with X-ray CCD cameras on-board ASCA (Kaneda et al. 1997) and Chandra (Ebisawa et al. 2005). These instruments revealed that the line centroid energies in the GRXE are systematically lower than 6.7 keV (the energy expected from He-like ion in thermal equilibrium plasma), which imply that either the line emission is from non-ionization equilibrium plasma or there is an additional 6.4 keV fluorescent line emission. Suzaku, for the first time, resolved the GRXE iron line emission into three narrow lines, ones from neutral or low ionized (6.4 keV), He-like (6.7 keV), and H-like (7.0 keV) ions (Ebisawa et al. 2008), concluding that the GRXE iron line emission is both from hot thermal plasmas and fluorescence by cold materials.

Regarding the origin of the GRXE, there is a strong argument in favor of collection of faint point sources as opposed to the diffused emission (e.g., Revnivtsev et al. 2006; Krivonos et al. 2007; Revnivtsev et al. 2009; Revnivtsev et al. 2010 and references therein), although the question remains "what are these Galactic point sources?" Candidate point sources for the GRXE are cataclysmic variables (CVs) and active binaries (ABs). CVs are known to have such strong emission lines and hard spectra, but most of them are brighter than $\sim 10^{31}$ erg s^{-1}, and their population may not be sufficient to account for all the GRXE. Revnivtsev et al. (2009) proposed that ABs dimmer than $\sim 10^{31}$ erg s^{-1} are likely candidates to account for the majority of the GRXE. However, ABs are well known to have thermal but much softer continuum spectra than CVs. Yuasa (2010) proposed that intermediate polars (IPs), which are a subclass of magnetic CVs (mCVs), are main sources of the hard X-ray emission of the GRXE, giving support to the point source scenario for the origin of the GRXE. Yuasa (2010) concluded that combination of IPs and ABs will explain most of the 6.7 keV and 7.0 keV emission lines in the GRXE as well as the continuum emission above 20 keV, whereas an *ad hoc* additional 6.4 keV line component is needed to explain the entire GRXE by the point source model.

This X-ray fluorescence is, on the other hand, believed by some authors to be due to irradiation of the molecular clouds by X-ray photons or it may be as result of cosmic-ray particle bombardment (Koyama et al. 1986; Dogiel et al. 1998; Murakami et al. 2000; Valinia et al. 2000; Koyama et al. 2007; Yusef-Zadeh et al. 2007; Dogiel et al. 2009; Capelli et al. 2011). This is also likely, since Galactic γ-ray *diffuse* emission above $\sim$100 keV is successfully explained by the cosmic-rays and interstellar matter interaction model (e.g., Strong et al. 2005).

In this paper, we study origin of the 6.4 keV emission line in the GRXE, examining if this emission could be fully resolved by collection of point sources. We focused on hard X-ray emitting symbiotic stars (hSSs) and magnetic CVs (mCVs) observed with the Suzaku satellite (Mitsuda et al. 2007), since they are known to be significant 6.4 keV line emitters (e.g., Ezuka & Ishida 1999; Yuasa et al. 2010; Luna & Sokoloski 2007; Smith et al. 2008; Kennea et al. 2009; Eze 2011). We studied 4 hSSs and 19 mCVs (one polar and 18 IPs), all observed with the Suzaku satellite, and estimated their contributions to the 6.4 keV line emission flux of the GRXE. Our goal is to determine if they are the main sources of the GRXE 6.4 keV line emission flux, or if some additional sources are required.

2 Data Selection

Our target sources, hSSs and mCVs, were selected based on the fact that they have been observed with Suzaku and have strong Fe Kα emission lines with hard X-ray emission above 20 keV. All the four hard X-ray emitting symbiotic stars, SS73 17, RT Cru, T CrB, and CH Cyg observed with Suzaku were selected. In selecting the mCVs (polars and IPs), we used a CV catalog (Ritter & Kolb 2003) and the IP catalog[1]. Five sources in the catalog, AE Aqr, AM Her, GK Per, 1RXS J070407.9+26250, and 1RXS J180340.0+40121 were dropped, even though observed with Suzaku, because they appear to had been too faint during their observations or have particular emission mechanism (AE Aqr: e.g., Wynn et al. 1997). A total of 23 sources were thus selected (table 1).

3 Data Analysis and Results

Analysis of our data were done using version 2 of the standard Suzaku pipeline products, and the HEASoft[2] version 6.10. In majority of the sources we used $250''$ radius to extract all events for the XIS detector for the production of the source spectra but in some cases where the $250''$ radius overlaps with the calibration sources at the corners, we adjusted the radius accordingly. The XIS background spectra were extracted with $250''$ radius with no apparent sources and were offset from both the source and corner calibrations. The radius was also adjusted accordingly in some cases where it overlaps with the calibration sources at the corners. Response Matrices File and Ancillary Response File were generated for the XIS detector using the FTOOLS `xisrmfgen` and `xissimarfgen` (Ishisaki et al. 2007), respectively. Suzaku XIS 0, 2, and 3 have front-illuminated (FI) chips with similar features, so we merged the spectra of XIS 0 and 3, which we hereafter refer to as XIS FI (XIS 2 has been out of service since November 9, 2006 due to an anomaly). XIS 1 is back-illuminated (BI), and we hereafter refer it to as XIS BI.

In the HXD PIN detector analysis, we used the non-X-ray background files and response matrix files appropriate for each observation provided by the Suzaku team. We used the `mgtime` FTOOLs to merge the good time intervals to get a common value for the PIN background and source event files. The source and background spectra extraction were done for each observa-

[1] http://asd.gsfc.nasa.gov/Koji.Mukai/iphome/catalog/alpha.html
[2] See http://heasarc.gsfc.nasa.gov/lheasoft/ for details.

tion using the `xselect` filter time file routine. We corrected for the dead time of the observed spectra using the `hxddtcor` in the Suzaku FTOOLS. According to the standard analysis procedure, exposure time for all observations for the derived background spectra were increased by a factor of 10 to take care of the event rate in the PIN background event file which is made 10 times higher than the real background for suppression of the Poisson errors. We assumed a cosmic background model obtained with the HEAO-1 satellite (Boldt 1987).

Spectral analysis of all observations were performed using XSPEC version 12.7. We modeled the spectrum using absorbed bremsstralung model with three Gaussian lines for the three Fe Kα emission lines to measure the iron line fluxes. We assumed two types of absorption by full-covering and partial covering matter. Since we were primarily interested in the ion lines, our fitting covers 3–10 keV for the XIS BI, 3–12 keV for the XIS FI and 15–40 keV for the HXD PIN. We ignored energy range below 3 keV in the XIS FI and BI detector to avoid intrinsic absorption which is known to affect data at this energy range, and energies above 10 keV were ignored for XIS BI because the instrument background is higher compared to the XIS FI detectors. We also ignored energy range above 40 keV in the HXD PIN detector in order to obtain high signal-to-noise ratio signals.

The three Fe lines, neutral or low ionized (6.4 keV), He-like (6.7 keV), and H-like (7.0 keV) ions, were clearly resolved in all the sources except IGR J17303–0601 where we were unable to detected the H-like (7.0 keV) significantly but the other two lines were detected. Spectra of all the sources can be found in an earlier work by Eze (2015) and spectral parameters were shown in table 2.

Furthermore, in order to determine average spectra of the hSSs and the mCVs, we used `addascaspec` to average the spectra of hSSs and mCVs (as well as responses). We used the same model to produce the spectra for the average hSSs and average mCVs. The spectra and spectral parameters for the average hSSs and average mCVs were presented in figure 1 and table 2, respectively.

We detected strong 6.4 keV iron line emission in the average hSSs spectrum with an equivalent width (EW) of 179^{+46}_{-11} eV and in the average mCVs spectrum with 93^{+20}_{-3} eV. We have found that the 6.4 keV line EW is much stronger in hSSs than in mCVs, which suggests that hSSs can be strong candidates of the GRXE 6.4 keV line emission. For comparison, 6.4 keV iron line EWs of the GRXE are of 90–390 eV, depending on the Galactic locations (Yamauchi et al. 2009).

4 Discussion

4.1 The 6.4 keV Line Emission

The 6.4 keV fluorescence line emission is usually due to irradiation of the neutral (or low ionized) material (iron) by a hard X-ray source. Eze (2015) used these sources used in this work to study the origin of the 6.4 keV fluorescence line and found that the emission could be partly from the reflection of hard X-rays from the accretion disks/white dwarf surfaces and from the absorption column. Generally, for all compact objects that accretes matter such as white dwarfs, neutron stars, and black holes, there are often emission of the Fe Kα fluorescence line as well as Compton reflection which signifies presence of the surrounding cold matter.

hSSs and mCVs are both binary systems in which white dwarfs accrete matter from their companions. The CVs are semi-detached systems in which the secondary star fills its Roche lobe and starts transferring mass into the lobe of the compact white dwarf primary. The transferred material has too much angular momentum to fall directly onto the surface of the white dwarf, but instead builds an accretion disk, which spirals round the white dwarf (e.g., Warner 1995). On the other hand, SSs are interacting binaries formed from a red giant star and a hot degenerate companion which accretes mass from the stellar wind of the red giant. Such a nebulae often formed surrounding the system is typically detected via various optical emission lines, whereas accretion disks may not be formed (Kenyon 1986). Therefore, at least for hSSs, the 6.4 keV fluorescent emission lines are considered to be mainly from white dwarf surfaces. Hard X-rays emitted in the vicinity of the white dwarfs irradiate the white dwarf surfaces (e.g., Luna & Sokoloski 2007; Eze et al. 2010), leading to the emission of the Fe Kα fluorescence line.

We found that the EWs of the 6.4 keV line of hSSs are systematically higher than those of mCVs, such that the average EW of hSSs and mCVs are 179^{+46}_{-11} eV and 93^{+20}_{-3} eV, respectively (table 2). In order to see if hSSs are truly more efficient 6.4 keV line emitters than mCVs, we estimated 6.4 keV photon luminosities for those hSSs and mCVs whose distances are known (table 3). As a result, we found that the 6.4 keV line luminosities of hSSs are systematically higher than those of mCVs; that of the average hSSs is 9.2×10^{39} photons s^{-1}, and that of the average mCVs is 1.6×10^{39} photons s^{-1}. We note that one of the hSSs, RT Cru, has a high luminosity of 30×10^{39} photons s^{-1}, however, if we isolate this source, the average luminosity of hSSs will become 2.2×10^{39} photons s^{-1}, which will still be higher than that of the mCVs.

We suppose there is a reason why the 6.4 keV line luminosities of hSSs are significantly higher than those of mCVs, even though hSSs may lack accretion disks. Many hSSs are believed to have a cocoon of gas coming from the red giant compan-

ion and surrounding the white dwarf (e.g., Luna & Sokoloski 2007; Eze et al. 2010; Eze 2011). Hence, there is a possibility that the additional 6.4 keV line emission is from irradiation of the thick cold absorbing circumstellar gas partially covering the hard X-ray source. In fact, our spectral analysis indicate that the average hSSs spectrum has significantly higher hydrogen circumstallar partial covering fraction of 0.70 ± 0.01, compared to that of the average mCVs, 0.44 ± 0.01 with similar hydrogen column density of partial covering matter (table 2).

4.2 The Contribution of the 6.4 keV Line Emission of hSSs and mCVs to that of the GRXE

If the Galactic 6.4 keV line source has the line luminosity ($L_{6.4}$ photons s^{-1}) and number the density (n cm^{-3}), the 6.4 keV line emissivity may be expressed as

$$\frac{nL_{6.4}}{4\pi} \text{ photons s}^{-1} \text{ cm}^{-3} \text{ str}^{-1} \quad (1)$$

and the observed 6.4 keV line flux in photons s^{-1} cm^{-2} str^{-1} will be

$$F_{6.4} = \int \frac{n\,(x)\,L_{6.4}}{4\pi} dx \approx \frac{\langle L_{6.4} \rangle}{4\pi} \int n(x) dx, \quad (2)$$

where the integration is made along the line of sight, and $\langle L_{6.4} \rangle$ is the average 6.4 keV line luninosity either from hSSs or mCVs (see also Yamauchi et al. 2009). In order to be precise, we will have to take into account luminosity functions of the hSSs and mCV to estimate $\langle L_{6.4} \rangle$. However, it is known that contribution of CVs to the GRXE is limited to a narrow range of the luminosities (e.g., Sazonov et al. (2006); Warwick (2014)). Thus, we approximate $\langle L_{6.4} \rangle$ with the values estimated in the previous section from the current Suzaku samples, $\langle L_{6.4} \rangle \sim 9.2 \times 10^{39}$ photons s^{-1} for hSSs and $\sim 1.6 \times 10^{39}$ photons s^{-1} for mCVs.

Let's consider the measurement of the 6.4 keV photon flux at the position $(l, b) \approx (28.5^\circ, 0^\circ)$, $(8 \pm 2) \times 10^{-5}$ photons s^{-1} cm^{-2} deg^{-2} ≈ 0.26 photons s^{-1} cm^{-2} str^{-1} (Ebisawa et al. 2008). We are going to estimate the contributions from mCVs using (2).

Following Sazonov et al. (2006); Revnivtsev & Sazonov (2007) and Warwick (2014), we take the model of the stellar mass distribution on the Galactic plane,

$$\rho = \rho_{0,disk} \exp\left[-\left(\frac{R_m}{R}\right)^3 - \frac{R}{R_{disk}} \right], \quad (3)$$

where R_m and R_{disk} represents the inner cut-off radius and e-fold disk radius, respectively. These authors claim that almost all the total GRXE flux is explained assuming the stellar density in the form of (3). However, we found that the three authors adopt slightly different disk size and normalization, while they use the same outer disk radius, R_{max} = 10 kpc: Sazonov et al. (2006) takes $\rho_{0,disk} = 0.61 M_\odot$ pc^{-3}, $R = 3$ kpc, $R_{disk} = 3$ kpc. Revnivtsev & Sazonov (2007) takes $\rho_{0,disk} = 5.5 M_\odot$ pc^{-3}, $R_m = 2.5$ kpc, R_{disk} 2.2 kpc. Warwick (2014) takes the same R_m and R_{disk} as Revnivtsev & Sazonov (2007), but $\rho_{0,disk} = 1.6 M_\odot$ pc^{-3}. Because of these differences, the total surface mass density integrated in the direction of $l = 28.5^\circ$ is significantly different: 1200 (Sazonov et al. 2006), 1900 (Warwick 2014) or 6700 (Revnivtsev & Sazonov 2007) $M_\odot$ pc^{-2} (see Fig. 2). This may not be very surprising, since only less than half of the GRXE is resolved into point sources in this direction (Ebisawa et al. 2005), and estimate of the number of remaining extremely dim stars has a large uncertainty. If we assume the expected spatial number density of CVs normalized by stellar mass, $1.2 \times 10^{-5} M_\odot^{-1}$ (Sazonov et al. 2006) we may calculate the expected 6.4 keV line photon flux from CVs; 0.19, 0.31 or 1.1 photons s^{-1} cm^{-2} str^{-1}, depending on the three different stellar mass density estimates. Obviously, the latter two are over-estimates, exceeding the observed value. In any case, we conclude that the observed 6.4 keV line photon flux in the direction of $l = 28.5^\circ$ may be explained totally by CVs, within the current uncertainty of the stellar densities.

What about the contribution from hSSs? We have very few number of known symbiotic stars 200 (Belczyński et al. 2000), of which only five are hSSs (see Kennea et al. (2009)). This makes it difficult to estimate the space density of the hSSs and we therefore require more discoveries of hSSs in the Galaxy in other to make a proper estimate of the space density. However, we believe that there are many more hSSs that are yet to be discovered, hence hSSs could contribute a significant percentage of the GRXE 6.4 keV line flux.

In summary, we conclude that the GRXE 6.4 keV line flux is primarily explained by mCVs. Contribution from the hSSs may not be neglected, since hSSs are intrinsically strong 6.4 keV line emitters. Taking account of contributions from other types of white dwarf X-ray binaries, the GRXE 6.4 keV line emission may be fully explained as being from a large number of accreting white dwarfs in the Galactic plane, most of which has yet to be identified.

In order to confirm our model, further work should be done to search for more, still dimmer 6.4 keV line emitting sources in the Galactic plane, which may be hSSs, mCVs, or other types of white dwarf binaries. We hope that next generation Galactic surveys by the incoming hard X-ray satellite missions such as Spectrum-Roentgen-Gamma" (SRG) satellite will detect a large number of such sources that would account for most of the GRXE 6.4 keV line emission.

We acknowledge the Suzaku team for providing data and some relevant files used in the analysis of this work. R. E. is very grateful to the Japan Society for the Promotion of Science (JSPS) for financial support under the JSPS Invitation Fellowship (Long Term), the Nigerian TETFund for National Research grant support and ISAS/JAXA, Sagamihara Campus for hosting him. This research made use of data obtained from Data ARchives and Transmission System (DARTS), provided

by Center for Science-satellite Operation and Data Archives (C-SODA) at ISAS/JAXA. Some part of this work were[3]

References

Barlow, E. J., Knigge, C., Bird, A. J., Dean, A. J., Clark, D. J., Hill, A. B., Molina, M., & Sguera, V. 2006, MNRAS, 372, 224

Belczyński, K., Mikolajewska, J., Munari, U., Ivison, R. J., & Friedjung, M. 2000, A&AS, 146, 407

Beuermann, K., Harrison, Th. E., McArthur, B. E., Benedict, G. F., & Gånsicke, B. T. 2003, A&A, 412, 821

Boldt, E. 1987, Phys. Rep., 146, 215

Bonnet-Bidaud, J. -M., de Martino, D., Falanga, M., Mouchet, M., & Masetti, N. 2007, A&A, 473, 185

Capelli, R., Warwick, R. S., Porquet, D., Gillessen, S., & Predehl, P. 2011, A&A, 530, A38

de Martino, D., Bonnet-Bidaud, J. -M., Mouchet, M., Gånsicke, B. T., Haberl, F., & Motch, C. 2006, A&A, 449, 115

Dogiel, V. A., Ichimura, A., Inoue, H., & Masai, K. 1998, PASJ, 50, 567

Dogiel, V. A., et al. 2009, PASJ, 61, 901

Ebisawa, K., et al. 2005, ApJ, 635, 214

Ebisawa, K., et al. 2008, PASJ, 60, S223

Eze, R. N. C., Luna, G, J, M., & Smith, R. K. 2010, ApJ, 709, 816

Eze, R. N. C. 2011, Adv. in Space Research, 47, 1999

Eze, R. N. C. 2015, New Astronomy, 37, 35

Ezuka, H., & Ishida, M. 1999, ApJS, 120, 277

Ishisaki, Y., et al. 2007, PASJ, 59, S113

Kaneda, H., Makishima, K., Yamauchi, S., Koyama, K., Matsuzaki, K., & Yamasaki, N. Y. 1997, ApJ, 491, 638

Kennea, J. A., Mukai, K., Sokoloski, J. L., Luna, G. J. M., Tueller, J., Markwardt, C. B., & Burrows, D. N. 2009, ApJ, 701, 1992

Kenyon, S. J. 1986, The symbiotic stars (Cambridge: Cambridge University Press)

Koyama, K., Makishima, K., Tanaka, Y., & Tsunemi, H. 1986, PASJ, 38, 121

Koyama, K., et al. 2007, PASJ, 59, S221

Krivonos, R., Revnivtsev, M., Churazov, E., Sazonov, S., Grebenev, S., & Sunyaev, R. 2007, A&A, 463, 957

Littlefair, S. P., Dhillon, V. S., & Marsh, T. R. 2001, MNRAS, 327, 669

Luna, G. J. M., Sokoloski, J., Mukai, K., & Nelson, T. 2010, Astron. Telegram, 3053

Luna, G. J. M., & Sokoloski, J. L. 2007, ApJ, 671, 741

Masetti, N. et al. 2006, A&A, 459, 21

McArthur, B. E., Benedict, G. F., Lee, J., et al. 2001, ApJ, 560, 907

Mitsuda, K. et al. 2007, PASJ, 59, S1

Murakami, H., Koyoma, K., Sakano, M., & Tsujimoto, M. 2000, ApJ, 534, 283

Revnivtsev, M., Sazonov, S., Gilfanov, M., Churazov, E., Sunyaev, R., 2006. A&A, 452, 169.

Revnivtsev, M. & Sazonov, S. 2007, A&A, 471, 159

Revnivtsev, M., Sazonov, S., Churazov, E., Froman, W., Vikhlinin, A., & Sunyaev, R. 2009, Nature, 458, 1142

Revnivtsev, M., van den Berg, M., Burenin, R., Grindlay, J. E., Karasev, D., & Forman, W. 2010, A&A, 515, A49

Ritter, H., & Kolb, U. 2003, A&A, 404, 301

Sazonov, S, Revnivtsev, M., Gilfanov, M., Churazov, E. & Sunyaev, R., 2006, A&A, 450, 117

Smith, R. K., Mushotzky, R., Mukai, K., Kallman, T., Markwardt, C. B., & Tueller, J. 2008, PASJ, 60, 43

Sokoloski, J. L., & Kenyon, S. J. 2003, ApJ, 584, 1021

Strong, A. W., Diehl, R., Halloin, H., Schnfelder, V., Bouchet, L., Mandrou, P., Lebrun, F., & Terrier, R. 2005, A&A, 444, 495

Suleimanov, V., Revnivtsev, M., & Ritter, H. 2005, A&A, 435, 191

Valinia, A., Tatischeff, V., Arnaud, K., Ebisawa, K., & Ramaty, R. 2000, ApJ, 543, 733

Warner, B. 1995, Cataclysmic variable stars (Cambridge: Cambridge University Press)

Warwick, R. S., Turner, M. J. L., Watson, M. G., & Willingale, R. 1985, Nature, 317, 218

Warwick, R. S. 2014, MNRAS, 445, 66

Worrall, D. M., Marshall, F. E., Boldt, E. A., & Swank, J. H. 1982, ApJ, 255, 111

Yamauchi, S., & Koyama, K. 1993, ApJ, 404, 620

Yamauchi, S., et al. 2009, PASJ, 61, S225

Yuasa, T., Nakazawa, K., Makishima, K., Saitou, K., Ishida, M., Ebisawa, K., Mori, H., & Yamada, S. 2010, A&A, 520, A25

Yuasa, T. 2010, Ph.D Thesis, University of Tokyo, Japan

Yusef-Zadeh, F., Wardle, M., & Roy, S. 2007, ApJ, 665, L123

Wynn, G. A., King, A. R., & Horne, K. 1997, MNRAS, 286, 436

[3] Reprinted from Publication of New Astronomy, Vol. 36(2015), Author: R.N.C., Eze, Title: On the origin of the iron fluorescent line emission from the Galactic Ridge/ Page No. 64 - 69, Copyright (2015), with permission from Elsevier

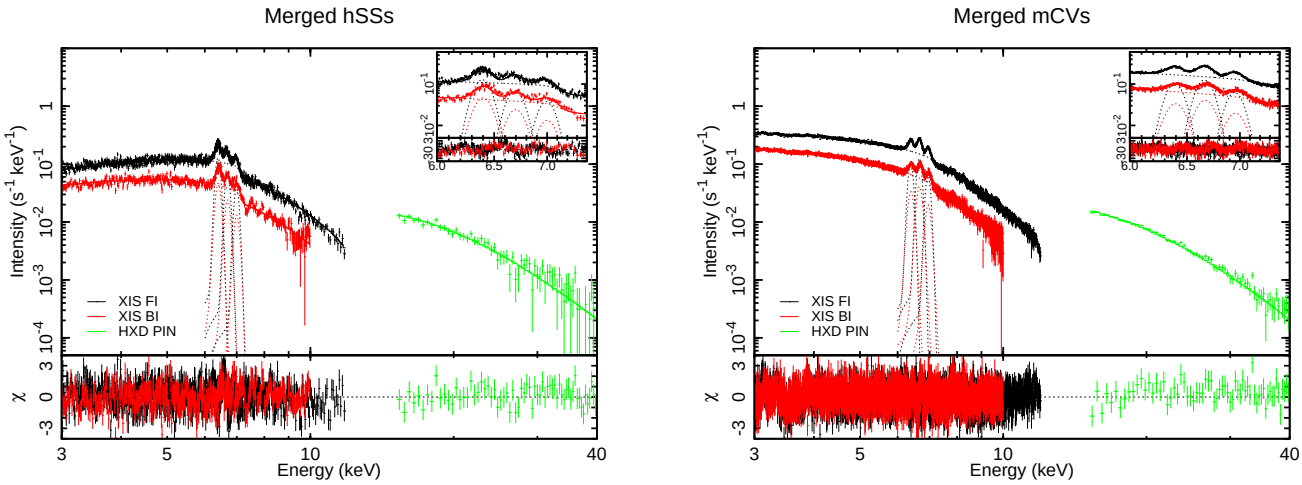

Fig. 1. Spectra of the average symbiotic stars and the average magnetic cataclysmic variables. In the upper panel, the data and the best-fit model are shown by crosses and solid lines, respectively. Each spectral component is represented by dotted lines. In the lower panel, the ratio of the data to the best-fit model is shown by crosses. The inset in the upper panel is an enlarged view for the Fe Kα complex lines.

??

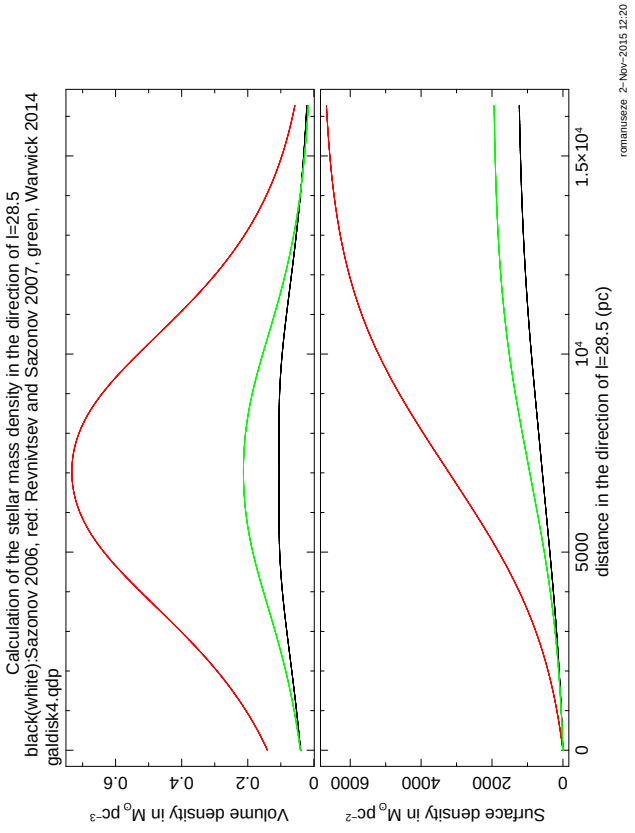
Calculation of the stellar mass density in the direction of l=28.5
black(white):Sazonov 2006, red: Revnivtsev and Sazonov 2007, green, Warwick 2014
galdisk4.qdp
romanuseze 2-Nov-2015 12:20
Volume density in M$_\odot$ pc^{-3}
Surface density in M$_\odot$ pc^{-2}
distance in the direction of l=28.5 (pc)

Fig. 2. Calculation of the stellar mass density

Table 1. The symbiotic stars, polars, and intermediate polars used in this work

Source Name	ObsID	Obs. start (UT) Date / Time	Exp. (ks)
Symbiotic Stars			
CH Cyg	400016020	2006-05-28 / 07:28	35.2
T CrB	401043010	2006-09-06 / 22:44	46.3
RT Cru	402040010	2007-07-02 / 12:38	50.9
SS73 17	403043010	2008-11-05 / 16:30	24.9
Polars			
V1432 Aql	403027010	2008-04-16 / 21:33	24.9
Intermediate Polars			
NY Lup	401037010	2007-02-01 / 15:17	86.8
RX J2133.7+5107	401038010	2006-04-29 / 06:50	62.8
EX Hya	402001010	2007-07-18 / 21:23	91.0
V1223 Sgr	402002010	2007-04-13 / 11:31	46.2
MU Cam	403004010	2008-04-14 / 00:55	50.1
V2400 Oph	403021010	2009-02-27 / 11:42	110.0
YY Dra	403022010	2008-06-15 / 18:37	27.4
TV Col	403023010	2008-04-17 / 18:00	30.1
V709 Cas	403025010	2008-06-20 / 10:24	33.3
IGR J17303−0601	403026010	2009-02-16 / 10:09	27.7
IGR J17195−4100	403028010	2009-02-18 / 11:03	26.9
BG CMi	404029010	2009-04-11 / 12:11	45.0
PQ Gem	404030010	2009-04-12 / 13:46	43.2
TX Col	404031010	2009-05-12 / 19:19	51.1
FO Aqr	404032010	2009-06-05 / 08:14	33.4
AO Psc	404033010	2009-06-22 / 11:50	35.6
IGR J00234+6141	405022010	2010-06-25 / 00:06	77.4
XY Ari	500015010	2006-02-03 / 23:02	93.6

Table 2. The Fe lines fit parameters.*

Source Name	$N_{\rm H}^{\rm f}$	$N_{\rm H}^{\rm p}$	C	kT	$F_{\rm cont}$	$E_{6.4}$	$F_{6.4}$	EW$_{6.4}$	$E_{6.7}$	$F_{6.7}$	EW$_{6.7}$	$E_{7.0}$	$F_{7.0}$	EW$_{7.0}$
Symbiotic Stars														
CH Cyg	22.0 ± 7.0	99^{+26}_{-37}	0.91 ± 0.04	6^{+3}_{-2}	9.2 ± 0.5	6.41 ± 0.02	20.2 ± 0.6	580^{+424}_{-65}	6.59 ± 0.05	5.9 ± 1.8	111^{+95}_{-35}	$6.81^{+0.12}_{-0.07}$	1.8 ± 0.7	66^{+87}_{-38}
T CrB	17.7 ± 2.2	37 ± 6	0.71 ± 0.06	19^{+3}_{-2}	14.7 ± 1.3	6.43 ± 0.01	9.6 ± 0.6	117^{+48}_{-46}	6.72 ± 0.02	6.5 ± 0.5	85^{+40}_{-12}	7.01 ± 0.02	5.3 ± 0.3	104^{+38}_{-41}
RT Cru	3.3 ± 0.4	58 ± 9	0.46 ± 0.05	29^{+9}_{-5}	12.0 ± 1.1	6.38 ± 0.01	11.0 ± 0.9	174^{+38}_{-30}	6.64 ± 0.01	5.8 ± 0.5	52^{+34}_{-15}	6.96 ± 0.01	3.2 ± 0.3	51^{+17}_{-25}
SS73 17	9.2 ± 0.5	34 ± 5	0.65 ± 0.05	38 ± 6	4.9 ± 1.0	6.38 ± 0.01	7.6 ± 0.6	185^{+120}_{-63}	6.67 ± 0.01	7.7 ± 0.2	158^{+136}_{-41}	6.95 ± 0.01	4.4 ± 0.1	93^{+116}_{-40}
Polars														
V1432 Aql	3.0 ± 0.5	61 ± 9	0.56 ± 0.05	15 ± 3	$14.7^{+3.8}_{-2.9}$	6.42 ± 0.01	6.5 ± 0.7	91^{+33}_{-20}	6.67 ± 0.02	5.5 ± 0.5	84^{+40}_{-8}	7.00 ± 0.03	2.0 ± 0.4	42^{+29}_{-34}
Intermediate Polars														
NY Lup	0.6 ± 0.5	32 ± 8	0.35 ± 0.03	40 ± 7	$9.6^{+0.5}_{-0.3}$	6.40 ± 0.01	7.1 ± 0.3	118^{+34}_{-12}	6.66 ± 0.01	5.9 ± 0.3	94^{+43}_{-9}	6.94 ± 0.01	4.7 ± 0.2	70^{+28}_{-17}
RX J2133.7+5107	2.3 ± 0.3	73 ± 10	0.46 ± 0.05	29^{+10}_{-6}	8.9 ± 0.9	6.42 ± 0.01	6.3 ± 0.5	147^{+46}_{-26}	6.68 ± 0.02	3.1 ± 0.3	52^{+32}_{-14}	6.98 ± 0.02	2.3 ± 0.3	57^{+16}_{-26}
EX Hya	0.7 ± 0.5	98 ± 16	0.54 ± 0.06	10 ± 1	20.8 ± 0.1	6.41 ± 0.01	3.3 ± 0.2	28 ± 3	6.66 ± 0.02	2.9 ± 0.3	32 ± 1	6.95 ± 0.01	1.1 ± 0.3	109^{+5}_{-4}
V1223 Sgr	2.3 ± 0.2	72 ± 5	0.41 ± 0.03	25 ± 3	34.5 ± 0.3	6.38 ± 0.01	15.7 ± 0.7	89^{+17}_{-8}	6.67 ± 0.01	11.3 ± 0.6	59^{+18}_{-8}	6.95 ± 0.01	8.3 ± 0.5	45^{+14}_{-12}
MU Cam	1.8 ± 1.3	35 ± 14	0.48 ± 0.06	29^{+14}_{-8}	$3.6^{+0.8}_{-0.4}$	6.41 ± 0.01	2.9 ± 0.3	160^{+70}_{-32}	6.68 ± 0.02	2.5 ± 0.2	104^{+71}_{-22}	6.98 ± 0.01	2.4 ± 0.2	102^{+58}_{-36}
V2400 Oph	1.4 ± 0.2	64 ± 7	0.36 ± 0.04	18 ± 2	16.8 ± 0.3	6.39 ± 0.01	9.7 ± 0.5	112^{+26}_{-10}	6.68 ± 0.01	7.1 ± 0.3	77^{+24}_{-7}	6.96 ± 0.01	4.7 ± 0.3	57^{+20}_{-13}
YY Dra	1.1 ± 0.1	102^{+28}_{-30}	0.52 ± 0.08	17 ± 1	8.2 ± 0.1	6.41 ± 0.02	2.2 ± 0.3	49^{+34}_{-22}	6.69 ± 0.01	6.6 ± 0.4	157^{+52}_{-19}	6.99 ± 0.02	4.4 ± 0.4	173^{+63}_{-92}
TV Col	4.1 ± 0.2	36 ± 7	0.34 ± 0.05	27 ± 2	13.6 ± 1.2	6.41 ± 0.01	8.7 ± 0.3	114^{+39}_{-12}	6.69 ± 0.02	9.7 ± 0.2	122^{+45}_{-11}	6.98 ± 0.01	6.7 ± 0.1	99^{+41}_{-21}
V709 Cas	0.5 ± 0.4	51 ± 18	0.26 ± 0.07	26^{+7}_{-5}	$11.2^{+2.0}_{-1.3}$	6.41 ± 0.02	6.3 ± 0.5	108^{+33}_{-18}	6.69 ± 0.02	2.8 ± 0.4	56^{+29}_{-15}	6.99 ± 0.02	2.8 ± 0.3	48^{+27}_{-24}
IGR J17303−0601	1.9 ± 0.7	106^{+25}_{-28}	$0.56^{+0.09}_{-0.12}$	29 ± 7	10.5 ± 1.7	6.39 ± 0.02	4.6 ± 0.7	89^{+20}_{-16}	6.67 ± 0.04	2.3 ± 0.5	45^{+18}_{-13}	—	—	—
IGR J17195−4100	1.4 ± 0.1	21^{+8}_{-5}	0.27 ± 0.02	26 ± 5	$9.6^{+0.2}_{-0.5}$	6.40 ± 0.01	5.9 ± 0.4	113^{+40}_{-20}	6.69 ± 0.01	4.9 ± 0.4	90^{+39}_{-17}	6.97 ± 0.02	4.0 ± 0.4	82^{+40}_{-26}
BG CMi	$5.4^{+2.9}_{-1.0}$	43 ± 24	0.39 ± 0.09	19^{+5}_{-4}	$8.8^{+2.7}_{-1.4}$	6.40 ± 0.02	3.6 ± 0.4	86^{+17}_{-15}	6.65 ± 0.03	2.4 ± 0.3	57^{+23}_{-14}	7.00 ± 0.04	1.3 ± 0.3	39^{+23}_{-14}
PQ Gem	2.0 ± 0.4	64 ± 13	0.46 ± 0.07	18 ± 6	7.7 ± 0.2	6.39 ± 0.01	5.0 ± 0.6	137^{+28}_{-39}	6.66 ± 0.03	1.7 ± 0.4	32^{+60}_{-25}	6.93 ± 0.04	1.1 ± 0.4	23^{+37}_{-23}
TX Col	1.8 ± 0.6	59 ± 16	0.50 ± 0.08	12^{+4}_{-3}	$5.2^{+0.3}_{-0.1}$	6.38 ± 0.02	1.6 ± 0.3	47^{+51}_{-33}	6.68 ± 0.02	2.4 ± 0.3	83^{+71}_{-30}	6.95 ± 0.02	1.6 ± 0.2	49^{+52}_{-36}
FO Aqr	10.2 ± 0.2	143^{+56}_{-25}	0.61 ± 0.07	27 ± 2	37.0 ± 1.0	6.37 ± 0.01	28.4 ± 1.0	149^{+39}_{-30}	6.65 ± 0.01	16.6 ± 1.0	80^{+33}_{-54}	6.92 ± 0.02	11.1 ± 1.0	49^{+26}_{-22}
AO Psc	4.2 ± 0.2	40 ± 5	0.57 ± 0.06	17 ± 1	$13.8^{+0.8}_{-0.1}$	6.37 ± 0.01	8.9 ± 0.3	91^{+38}_{-16}	6.66 ± 0.02	13.0 ± 0.2	136^{+47}_{-16}	6.94 ± 0.01	7.4 ± 0.2	59^{+24}_{-21}
IGR J00234+6141	0.4 ± 0.5	32 ± 6	0.30 ± 0.04	24 ± 7.2	$2.1^{+1.6}_{-0.4}$	6.40 ± 0.03	1.2 ± 0.2	111^{+87}_{-39}	6.65 ± 0.04	6.2 ± 0.1	49^{+102}_{-36}	6.97 ± 0.03	0.6 ± 0.1	60^{+97}_{-43}
XY Ari	6.9 ± 0.2	26 ± 4	0.49 ± 0.05	28 ± 4	5.1 ± 0.6	6.39 ± 0.01	2.5 ± 0.7	85^{+32}_{-15}	6.68 ± 0.01	3.1 ± 0.3	112^{+33}_{-12}	6.97 ± 0.01	1.7 ± 0.4	72^{+31}_{-17}
Merged Spectra														
Merged hSSs	5.6 ± 0.2	50 ± 2	0.70 ± 0.01	20 ± 1	10.7 ± 1.3	$6.408^{+0.002}_{-0.005}$	7.7 ± 0.7	179^{+46}_{-11}	6.671 ± 0.007	5.2 ± 0.3	88^{+43}_{-8}	$6.969^{+0.013}_{-0.008}$	3.8 ± 0.3	74^{+28}_{-17}
Merged mCVs	1.6 ± 0.1	66 ± 1	0.44 ± 0.01	18 ± 1	12.3 ± 0.4	$6.403^{+0.003}_{-0.001}$	5.8 ± 0.1	93^{+20}_{-3}	$6.671^{+0.001}_{-0.002}$	7.7 ± 0.1	114^{+11}_{-4}	$6.957^{+0.003}_{-0.002}$	4.2 ± 0.1	62^{+7}_{-4}

* Parameters are the hydrogen column density of the full-covering and the partial-covering matter in units of 10^{22} cm^{-2} ($N_{\rm H}^{\rm f}$ and $N_{\rm H}^{\rm p}$), the covering fraction of the partial-covering matter (C), the continuum temperature in keV (kT), the continuum flux in 10^{-3} photons s^{-1} cm^{-2} ($F_{\rm cont}$), the center energies of 6.4, 6.7, and 7.0 keV lines in keV ($E_{6.4}$, $E_{6.7}$, and $E_{7.0}$), the line fluxes in 10^{-5} photons s^{-1} cm^{-2} ($F_{6.4}$, $F_{6.7}$, and $F_{7.0}$), and the equivalent widths in eV (EW$_{6.4}$, EW$_{6.7}$, and EW$_{7.0}$). EX Hya and YY Dra do not have both absorptions ($N_{\rm H}^{\rm f}$ and $N_{\rm H}^{\rm p}$), IGR J17195−4100 has no $N_{\rm H}^{\rm f}$, while TV Col and FO Aqr have no $N_{\rm H}^{\rm p}$.

Table 3. 6.4 keV line luminosities of the sources.*

Source Name	Luminosity (10^{39} photons s^{-1})	Distance (pc)	Ref.
Symbiotic Stars			
CH Cyg	1.52	250	[1]
T CrB	2.90	500	[2]
RT Cru	30.0	1500	[3]
SS73 17	2.29	500	[4]
Polars			
V1432 Aql	0.42	230	[5]
Intermediate Polars			
NY Lup	6.05	840	[5, 6]
RX J2133.7+5107	—	—	—
EX Hya	0.02	65	[7]
V1223 Sgr	5.27	527	[2, 7]
MU Cam	—	—	—
V2400 Oph	2.93	500	[8]
YY Dra	0.06	155	[9]
TV Col	1.44	370	[10]
V709 Cas	0.48	250	[6]
IGR J17303−0601	—	—	—
IGR J17195−4100	0.09	110	[11]
BG CMi	1.10	500	[9]
PQ Gem	0.97	400	[9]
TX Col	0.48	500	[9]
FO Aqr	5.50	400	[8]
AO Psc	0.67	250	[9]
IGR J00234+6141	0.41	530	[12]
XY Ari	0.22	270	[13]
Average Spectra			
hSSs Average	9.20	—	—
mCVs Average†	1.63	—	—

* References for the source distance: [1] Sokoloski & Kenyon (2003); [2] Kennea et al. (2009); [3] Luna & Sokoloski (2007); [4] Smith et al. (2008); [5] de Martino et al. (2006); [6] Balow et al. (2006); [7] Beuerman et al. (2003); [8] Suleimanov et al. (2005); [9] **?**; [10] McArthur et al. (2001); [11] Masetti et al. (2006); [12] Bonnet-Bidaud et al. (2007); [13] Littlefair et al. (2001).

† There are no estimated distances for RX J2133.7+5107, MU Cam, and IGR J17303−0601, hence they were not considered in the estimation of the average luminosity of the mCVs.